

Methodology to locate and quantify radial winding deformation in power transformers

Steven D. Mitchell ✉, James S. Welsh

School of Electrical and Computer Engineering, University of Newcastle, Callaghan, N.S.W 2308, Australia
 ✉ E-mail: steve.mitchell@newcastle.edu.au

ISSN 2397-7264

Received on 12th November 2016

Revised on 23rd January 2017

Accepted on 29th January 2017

doi: 10.1049/hve.2016.0085

www.ietdl.org

Abstract: Frequency response analysis (FRA) is a tool that can be used to detect changes within the structural geometry of a transformer. One application of FRA is to detect winding displacement after the transformer experiences an overcurrent event. This paper proposes a methodology which will facilitate both locating and quantifying winding deformation. The procedure is based on the fitting of a Gray Box transformer model to FRA measurements which were recorded both before and after the fault. Subtle variation in key parameters of the model can then be used to quantify winding deformation severity. The research will demonstrate the applicability of this approach to a wide range of transformer applications by using FRA from a modified 1.3 MVA distribution transformer, and assessing the change in key parameters relative to the emulated buckling introduced to the windings. The authors propose that this approach is ideally suited for use within an automated diagnostic system which will locate, diagnose and quantify winding deformation within power transformers.

1 Introduction

A significant proportion of the world's power transformers are approaching the end of their design life and because of pressure to reduce expenditure on infrastructure, many are operating beyond this milestone [1, 2]. A problem with this scenario is that the failure probability of a transformer increases significantly in the final quartile of a transformer's life [3], and in the event of a transformer failure, there is the potential for catastrophic consequences including loss of life and significant economic and environmental damage [4, 5]. It is therefore of critical importance that a transformer's condition is regularly monitored in order to pre-empt the need for maintenance, repair or replacement, particularly for the older members of a utility's transformer fleet.

A transformer winding's structural integrity can be compromised in many different ways. Some of the more common examples are system short circuits, mechanical shock during transportation to site or a reduction of winding clamping pressure over time [6, 7]. Under short circuit conditions, a transformer can experience severe electromagnetic forces on its winding structure [8]. Such forces can lead to winding deformation in both the axial and radial directions, which in turn can lead to transformer failure.

Historically, winding movement and deformation problems have been difficult to detect [7]. The traditional method for detecting such changes to the transformer winding geometry has been via leakage inductance measurements [9, 10]. However whilst radial deformation will result in a detectable change in the leakage inductance, axial deformation has only a minor influence and hence this method lacks the required sensitivity.

Frequency response analysis (FRA), as introduced by Dick and Erven in 1978 [11], has become the diagnostic method of choice for the detection of winding movement and deformation [6, 7, 12]. An FRA test is based around the injection of a signal into one terminal whilst measuring the response at another. There are two methods commonly used for the signal injection [13]. The first is the swept-frequency method or SFRA, which injects a variable frequency or white noise voltage. This approach has the highest signal to noise ratio. The second approach is the impulse method or IFRA, which directly injects a voltage impulse into the transformer terminals. This approach is currently receiving increased attention for its potential in online FRA applications [14].

By considering a transformer to be the electrical equivalent of a large distributed parameter network, each FRA test will yield a 'signature' unique to the transformer's mechanical geometry from the perspective of the input and output measurement terminal positions [15]. Any change in this 'signature' is indicative of a change in the transformer's geometry, hence its widespread application in the detection of winding movement and deformation. However in order to determine the change in an FRA 'signature' it is necessary for a comparison to be made against a suitable reference. The reference 'signature' is typically a historical version of the same FRA test, for example, the test results obtained during commissioning. However it can also be useful to compare measurements between different phases or from transformers of similar design [12].

FRA assessment is typically based on trained personnel visually comparing graphical representations of the transformer's frequency response or by using statistical methods such as correlation to quantify the degree of change [9, 10, 13]. Recently there has been a push to not just quantify change, but to interpret the underlying cause of the change directly from the frequency response [16]; to date this has not been satisfactorily achieved [10].

One approach to interpreting FRA data has been the application of Black Box modelling [17–19]. This approach is based on the development of mathematical models which accurately represent the frequency response between various terminal combinations. Any change in the FRA will result in model parameter changes which can then be interpreted for indications of a structural change within the transformer. Researchers such as Bigdeli [18, 19] have used neural networks to classify the fault relative to the change in parameters. Such an approach is dependent upon training data for different transformer topologies and their corresponding fault conditions. Outside of the laboratory such information may be difficult to obtain.

A recent and rather novel approach has been the application of radar imaging to determine winding deformation. This approach injects UHF impulses and interprets the results for structural change [20]. Challenges with this approach are due to the issues associated with the installation and positioning of the radar transmitters/receivers. UHF receivers are commonly fitted to a transformer's oil drain valves, which are fixed and limited in number [21].

An approach which has been adopted by many researchers has been the use of a transformer model based on its geometric parameters (White Box model) [15, 22, 23]. The rationale behind this approach is that a change in the geometry of a transformer will affect the physically representative parameters used in the model. A number of researchers in this area have been actively using transformer models to aid in the investigation of winding deformation. Research by Islam [24] investigated the sensitivity of model parameters on FRA. Deformation and displacement faults were simulated by modifying the model's series capacitance at various locations throughout the winding. Later research by Sofian *et al.* [25] demonstrated how the FRA of a deformed winding aligned with the simulated FRA from a transformer model whose parameters were analytically derived from the revised geometry. In the research by Jayasinghe *et al.* [26], changes were made to capacitance and inductance model parameters in order to simulate winding deformation. The results were then compared with those obtained from experimental methods. A similar approach was adopted by Tang *et al.* [27] to investigate the detection of minor winding deformation and displacement using higher frequency FRA measurements.

The parameters of such White Box transformer models are generally determined using finite element tools or precise analytical techniques [28, 29]. Such an approach requires detailed information on the internal geometry and material structure of the transformer which is not commonly available outside of the laboratory [30]. In earlier research published by the authors of this paper, a Gray Box transformer model was developed to support the interpretation of FRA [31]. Like the White Box model, the Gray Box model is based on the geometric parameters and material properties of the transformer, however many of the model parameters may be unknown and will need to be estimated by fitting the model's transfer function to external measurements. As a demonstration of the model's potential, the effect of varying levels of winding deformation on a transformer's FRA was simulated by changing appropriate parameter values within the transformer model. To date a number of other researchers have also used model simulation studies to investigate the effect of transformer winding deformation on FRA including [24, 32–36]. However a more robust evaluation of the effectiveness of a model in the detection of winding deformation, and the methodology implemented in this paper, is to test if the model parameters estimated directly from the FRA would correctly change to reflect a physically altered winding structure. This approach will facilitate quantifying the degree of deformation and identify which winding(s) are affected. The experimental validation of this approach is provided via buckle tests on a 1.3 MVA 11 kV/433 V Dyn1 distribution transformer.

This paper is structured in the following manner. Section 2 provides an overview of the generic phase model that is used in this research. Section 3 discusses how severe electromagnetic forces generated during a short circuit fault can result in different forms of winding deformation. This section also proposes a non-destructive methodology which can be used to emulate winding 'buckle' within a transformer. In Section 4 the winding buckle tests are conducted and the FRA results are analysed. In Section 5 the parameters are estimated by fitting the model to FRA and then comparing the results to those determined by finite element analysis (FEA). Concluding remarks are given in Section 6.

2 Review: generic phase transformer model

This section provides a brief review of the Gray Box model applied in this research. For more detailed information, please refer to [31].

2.1 Model structure

Transformer modelling is based on a rich history of research dating back over 100 years [37]. Building on this earlier work we have proposed using a generic n section lumped parameter model for

FRA analysis. The generic phase approach is particularly useful in FRA analysis due to the diverse range of tests and terminal combinations which may be connected. For example, for the high voltage (HV) winding end to end open circuit test [16] on a three-phase transformer there will be three tests comprised of the HV terminal combinations AC , BA and CB . For our model the generic HV terminals are designated X - Y - Z , and the corresponding low voltage (LV) terminals are x - y - z . The n section lumped parameter model for generic phase X is given in Fig. 1.

Each section of the HV and LV windings consists of the series combination of an inductive element \mathcal{L} and a resistive element \mathcal{R} . \mathcal{L} represents the frequency dependent self and mutual inductance relationships for a winding section. The term also takes into account the contribution of each winding section to the core losses associated with magnetic skin effect. The resistive element \mathcal{R} encapsulates the DC resistance and frequency dependent skin and proximity effects for a winding section. To account for the capacitance between windings, a capacitive element \mathcal{C}_{Xx} couples each equivalent winding section. The capacitance between turns and adjacent discs is modelled with the addition of \mathcal{C}_{SX} and \mathcal{C}_{Sx} , for the HV and LV windings, respectively. The capacitance between the LV winding and ground is given by \mathcal{C}_{gx} and the capacitance between the HV winding and the transformer tank walls is given by \mathcal{C}_{gX} . The capacitances \mathcal{C}_{XY} and \mathcal{C}_{ZX} represent the capacitance between adjacent HV windings. To accommodate for dielectric losses associated with the capacitive coupling of each element, the non-ideal capacitance elements are comprised of a

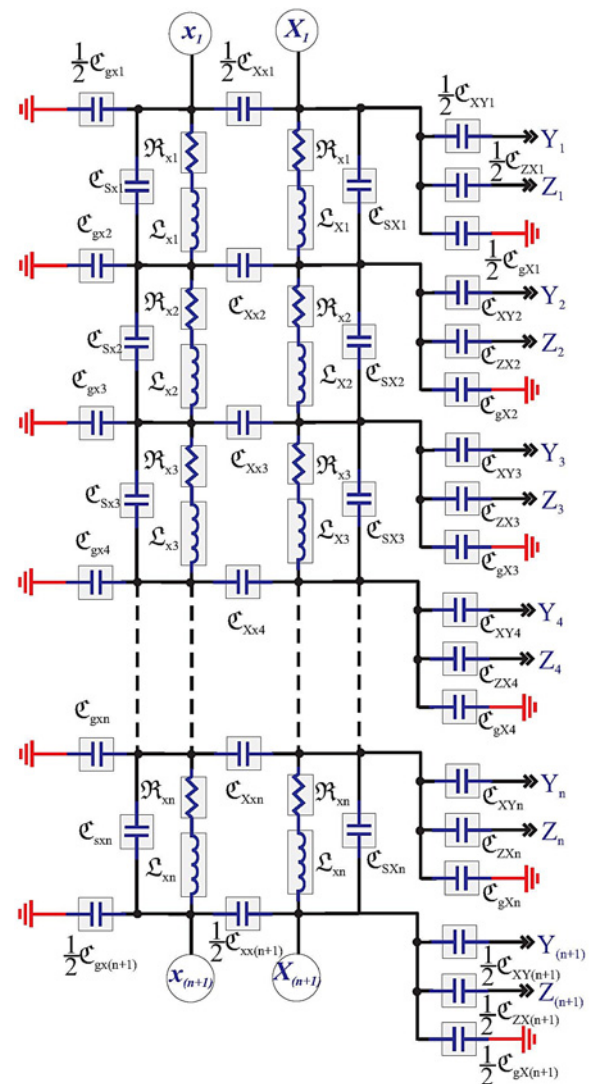


Fig. 1 Transformer model for generic phase X

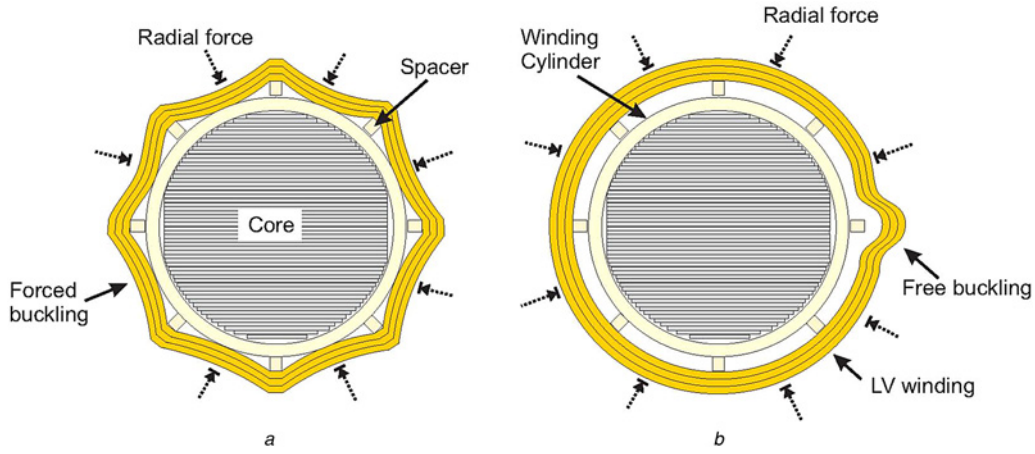


Fig. 2 Buckling modes associated with radial stress on a transformer's LV winding

a Forced buckling
b Free buckling

parallel combination of a frequency dependent resistance and an ideal capacitance.

2.2 Mathematical model

By assigning appropriate state variables and considering the model's mesh voltages and nodal currents, a state space representation of the three-phase transformer model can be derived for each of the FRA test topologies [38]. Taking the Laplace transform of the model's state space representation will give a transfer function of each of the FRA test topologies considered. This mathematical form can then be used to estimate the model parameters through curve fitting to the transformer FRA. This can be achieved through the application of a constrained optimisation algorithm which determines the model parameter values which minimise a cost function. The cost function utilised in this research takes the form,

$$J = J_H + J_L + J_{HL} \quad (1)$$

where

$$J_H = \left\| \log_{10} \left(\frac{\hat{G}_{AC}(s)}{H_{AC}(s)} \right) \right\|^2 + \left\| \log_{10} \left(\frac{\hat{G}_{BA}(s)}{H_{BA}(s)} \right) \right\|^2 + \left\| \log_{10} \left(\frac{\hat{G}_{CB}(s)}{H_{CB}(s)} \right) \right\|^2, \quad (2)$$

$$J_L = \left\| \log_{10} \left(\frac{\hat{G}_{an}(s)}{H_{an}(s)} \right) \right\|^2 + \left\| \log_{10} \left(\frac{\hat{G}_{bn}(s)}{H_{bn}(s)} \right) \right\|^2 + \left\| \log_{10} \left(\frac{\hat{G}_{cn}(s)}{H_{cn}(s)} \right) \right\|^2, \quad (3)$$

$$J_{HL} = \left\| \log_{10} \left(\frac{\hat{G}_{Aa}(s)}{H_{Aa}(s)} \right) \right\|^2 + \left\| \log_{10} \left(\frac{\hat{G}_{Bb}(s)}{H_{Bb}(s)} \right) \right\|^2 + \left\| \log_{10} \left(\frac{\hat{G}_{Cc}(s)}{H_{Cc}(s)} \right) \right\|^2. \quad (4)$$

In the cost function J , $H_{..}(s)$ represents the FRA data and $\hat{G}_{..}(s)$ the estimated transfer function for each of the considered three-phase FRA tests (HV winding end to end open circuit test, LV winding end to end open circuit test and capacitive interwinding test [16]). Please note that it is of critical importance that constraints be placed upon the model parameters in order to ensure that the estimator converges on an objective function that is physically representative of the transformer under test. This procedure is articulated in [30].

3 Short circuit forces and their potential consequences

A short circuit can place tremendous forces upon transformer windings and the mechanical structure [39]. Analysis of the leakage flux fields during a short circuit shows that the forces can be decomposed into radial and axial components [40]. The radial leakage flux is predominantly at the winding ends and produces an axial force on the windings. This can result in an axial displacement of the HV winding with respect to the LV winding [32]. The leakage flux which passes across the core window in the axial direction will produce an outward radial force on the HV winding and an inward radial force on the LV winding [40]. The outward radial force is tensile in nature and can stretch the conductor or break a poor joint, which can lead to failure. However, the relatively high-tensile strength of the conductor material means that failures in the outer winding due to tensile stress are unlikely [41]. The inward radial force places compressive stress on the LV winding. This compression can lead to winding deformation known as buckling and is a common mode of failure [32]. Buckling of the LV winding is the focus of this deformation study.

3.1 Buckling modes for the LV winding

When the support structure of the LV winding has a greater stiffness than the LV winding conductors themselves, under compressive stress it is possible for the winding conductors to bend in between each of the spacers towards the core. This is known as forced buckling [42] and is shown in Fig. 2a. Forced buckling in an LV winding will lead to an increase in the average distance between the HV and LV windings. This will result in a reduction in the HV to LV winding capacitance. Conversely, since the average distance between the LV winding and the core decreases, there is a corresponding increase in the LV to core capacitance [32]. These geometric changes will also subtly influence the leakage inductance characteristics [9].

Another buckling mode known as free buckling can occur when the conductor has a higher stiffness than the winding support structure. Under these circumstances the winding can buckle both inwards and outwards around the circumference [42]. This buckling mode is shown in Fig. 2b.

3.2 Emulation of an outward radial buckle in the LV winding

Due to the high capital costs associated with a transformer, it was necessary for the testing associated with this research to be

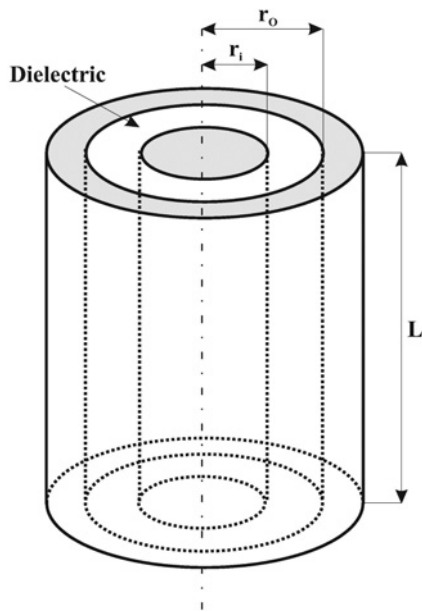


Fig. 3 Cylindrical capacitor

non-destructive. Therefore, to obtain the FRA data associated with different levels of winding deformation, we propose to utilise a method which could emulate ‘buckling’ in the LV winding, however would be temporary in nature so that the transformer can be restored to its original condition at the end of the testing program. Whilst noting that buckling will induce changes to a winding’s leakage inductance as well as its capacitance parameters, an induced change in capacitance can be more readily achieved in a non-destructive manner. Emulating the change in capacitance due to buckling of the LV winding requires the ability to reduce the HV to LV winding capacitance and increase the LV to core capacitance.

The capacitance between the HV and LV windings of a transformer can be estimated by treating it as a cylindrical capacitor (Fig. 3). Cylindrical capacitance is given by [43],

$$C = \frac{2\pi\epsilon L}{\ln[r_o/r_i]}, \quad (5)$$

where ϵ is the electrical permittivity of the dielectric medium between the two cylindrical conductors, L the cylinder length, r_o is the inside radius of the outer conductor and r_i is the outside radius

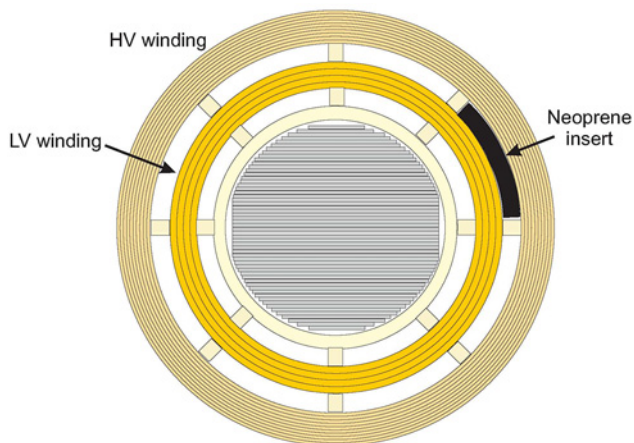


Fig. 4 Emulation of an outward radial buckle in the LV winding using a neoprene rubber insert between the HV and LV windings

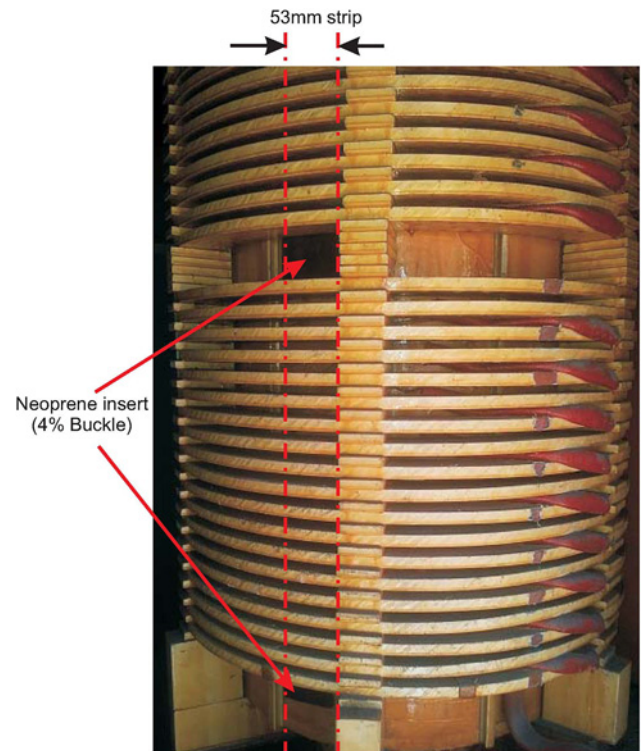


Fig. 5 Buckle emulated on phase A of a 1.3 MVA 11 kV/433 V transformer

of the inner conductor. Both the HV to LV winding capacitance and the LV to core capacitance can be estimated from the coaxial cylinder relationship of (5). With reference to (5), the only parameter that can be altered without significant mechanical change is ϵ , the electrical permittivity of the dielectric medium. A change in ϵ can be achieved by changing the dielectric material between the cylinders.

To facilitate the change in the electrical permittivity required to emulate ‘buckling’, neoprene rubber was inserted between the HV and LV windings of an air cooled transformer, as depicted in Fig. 4. Since neoprene rubber has an electrical permittivity of 6.7 (compared with 1 for air), the inserts will have the effect of increasing the HV to LV capacitance, and will therefore approximately emulate an outward radial buckle in the LV winding. Though a buckle in the LV winding would typically be inward, the objective set forth in this paper is to quantify the degree of radial winding deformation using FRA, be it in either the inward or outward direction.

4 Transformer ‘buckle’ tests

A 1.3 MVA 11 kV/433 V Dyn1 air cooled distribution transformer was used for the ‘buckle’ emulation modifications. The modifications involved the insertion of 6 mm neoprene rubber strips in between the phase A HV and LV windings. Each of the strips ran the full axial length of the winding as shown in Fig. 5. Four ‘buckle’ tests were conducted in total. The first test was an unmodified baseline test which is referred to as 0% ‘buckle’. For the second test the transformer was modified such that the neoprene inserts covered 8% of the LV winding’s outer circumference. This coverage was increased to 16% for the third test and to 24% for the fourth. HV winding end to end open circuit, LV winding end to end open circuit and capacitive interwinding FRA tests [16] were then conducted on each of the ‘buckle’ test cases. The resulting FRA tests for increasing levels of ‘buckling’ severity were recorded and a zoomed in view of their FRA responses is given in Figs. 6 and 7 (HV winding end to end open circuit and capacitive interwinding FRA tests, respectively).

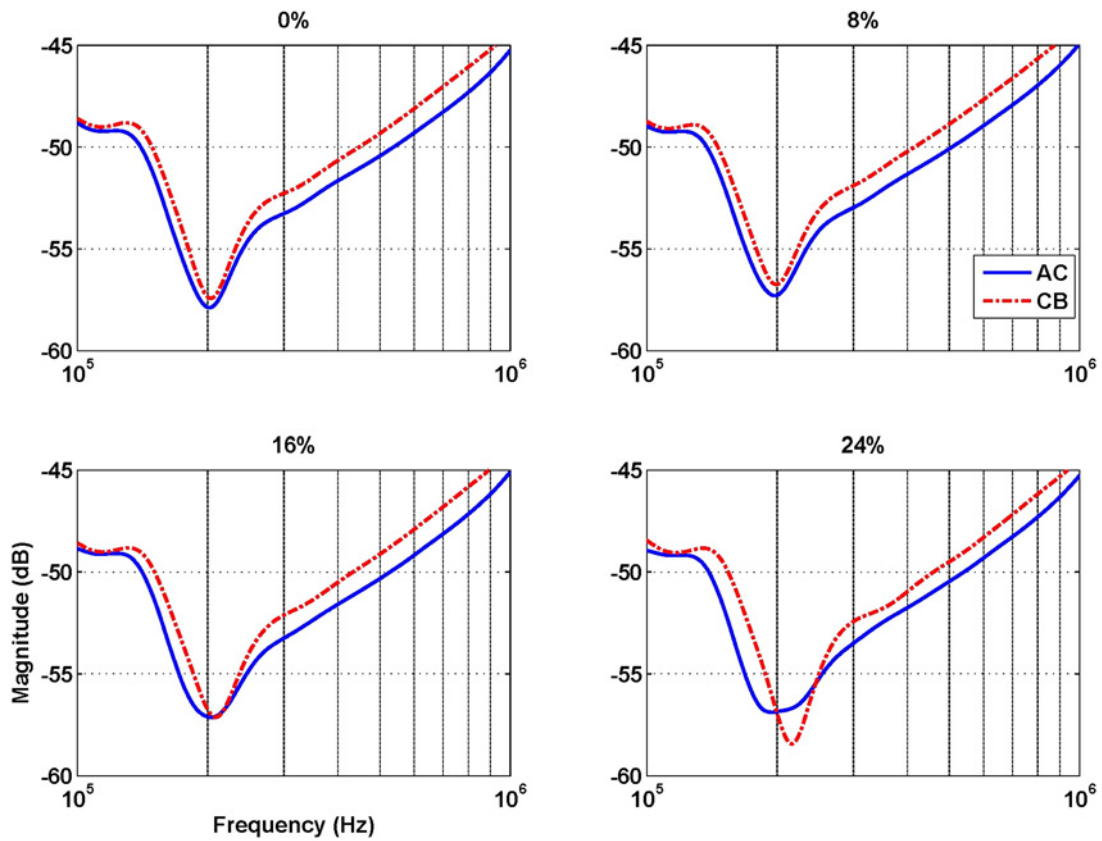


Fig. 6 Zoomed in view of the AC and CB HV end to end open circuit FRA tests. The tests are based on winding ‘buckling’ of 0, 8, 16 and 24%

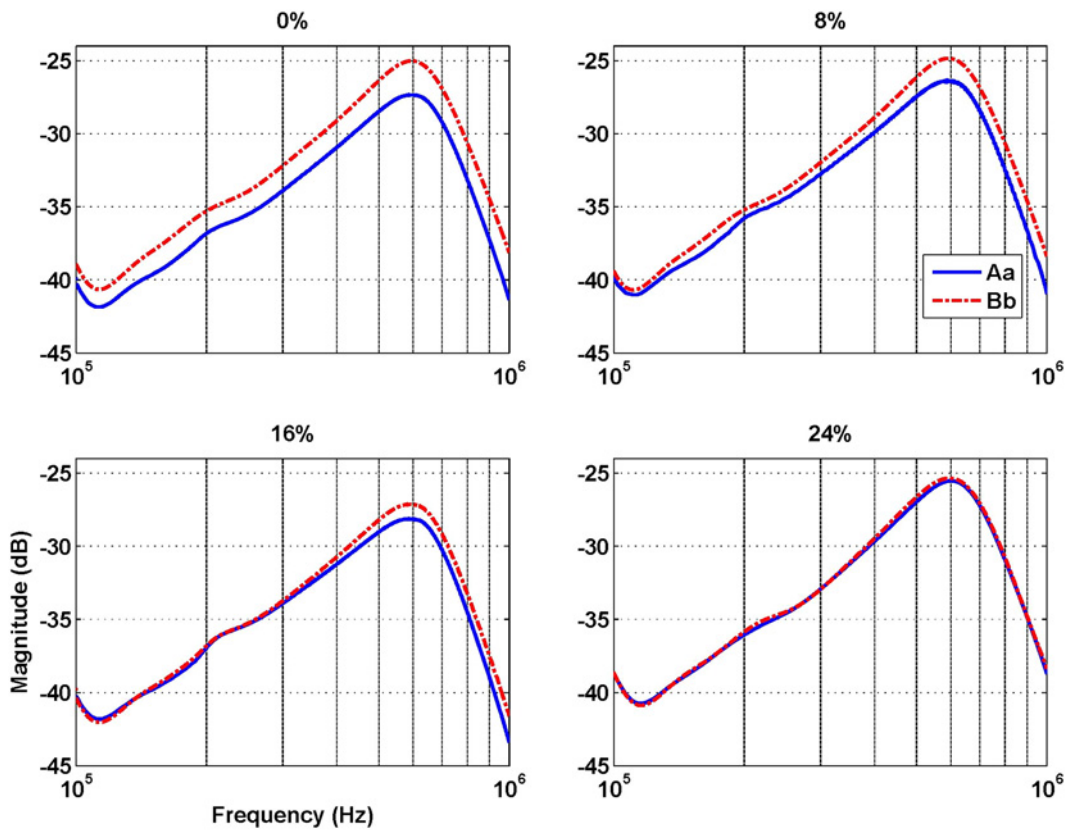


Fig. 7 Zoomed in view of Aa and Bb capacitive interwinding FRA tests. The tests are based on winding ‘buckling’ of 0, 8, 16 and 24%

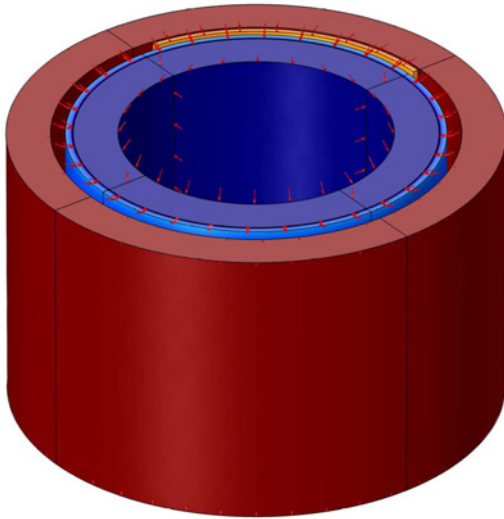


Fig. 8 FEA model of the emulated winding deformation

In each of these figures there is an observable change in the frequency response of windings associated with phase A of the transformer. As anticipated, the degree of change coincides with the increasing degree of ‘buckle’. Similar changes are also observed in the LV winding end to end open circuit FRA test results.

5 Parameter estimation for radial ‘buckling’

As discussed in Section 3.1, radial buckling results in changes to certain parameters. Given a baseline FRA for comparison (a baseline FRA would be equivalent to the FRA tests conducted after transformer installation and commissioning), knowledge of these parameters and the direction of their expected change can be used to our advantage. The first step is to run the estimation algorithm, using the cost function in (1), on the baseline FRA to determine the baseline parameter values. Other than the parameters specific to the deformation type being investigated, the remaining parameter values can all be fixed after this first run. The estimation algorithm is then re-run with the ‘buckled’ transformer FRA data. This approach significantly limits the degrees of freedom associated with the model, making the estimation algorithm more sensitive to the subtle parameter changes that are being investigated.

Whilst the air cooled transformer used in this research has the advantage of facilitating ready access to the windings, it is much more sensitive to atmospheric variations such as temperature and humidity which can vary widely throughout the course of a day of testing.

One area that is particularly sensitive to changes in both humidity and temperature is the losses associated with the permittivity of the insulation material. Variation in the complex permittivity results in changes in the resonant damping levels within the transformer’s frequency response [9]. As a result, the estimated parameter values may be influenced by changes in atmospheric conditions. To detect the subtle changes expected in the model parameters as a result of the ‘buckle’ tests, we need to adopt an approach which will minimise the influence of both temperature and humidity.

Table 1 ‘Buckling’ test interwinding capacitance estimates for each phase. All values are in pF

% ‘Buckling’	C_{Aai}	C_{Bbi}	C_{Cci}
0 (Baseline)	77.9	74.1	73.1
8	79.8	74.7	73.6
16	80.2	72.5	71.7
24	80.9	72.0	69.9

Table 2 Difference in interwinding capacitance for each of the ‘Buckling’ tests. All values in pF

% ‘Buckling’	$C_{Aai} - C_{Bbi}$	$C_{Aai} - C_{Cci}$	$C_{Bbi} - C_{Cci}$
0	+3.8	+4.8	+1.0
8	+5.1	+6.2	+1.1
16	+7.7	+8.5	+0.8
24	+8.9	+11.0	+2.1

Given a significant change in the temperature and absolute humidity associated with the transformer insulation, Ryder [12] advised using inter-phase comparisons to supplement those of the reference FRA. We have adopted this approach at a parameter level in the following manner. Rather than look at the absolute value of a parameter, we use the relative difference between similar parameters on different phases. An example is to monitor the relative difference between the interwinding capacitances i.e. $C_{Aai} - C_{Bbi}$ where C_{Aai} is the capacitance per model section between the HV and LV windings of phase A and C_{Bbi} capacitance per model section between the HV and LV windings of phase B. We use this difference as an *independent parameter* for each of the ‘buckle’ test cases. This differential approach removes the common mode effects due to changes in the atmospheric conditions since only the absolute value of the parameters is affected. Table 1 lists the algorithm’s interwinding capacitance estimates of each phase for each of the ‘buckle’ test cases. As expected, the changes observed in the capacitance are not always consistent due to atmospheric variations and model accuracy limitations. It was for this reason that the differential approach was proposed. Table 2 evaluates the difference in interwinding capacitance relative to each phase for each of the ‘buckling’ cases. It is clear that there is a proportional increase in the interwinding capacitance relative to the level of ‘buckling’ when phase A is considered (columns $C_{Aai} - C_{Bbi}$ and $C_{Aai} - C_{Cci}$); whereas the influence is not observed when the relative difference in the interwinding capacitance does not include phase A (column $C_{Bbi} - C_{Cci}$).

These results clearly indicate from a fault location perspective that the deformation is in the phase A winding structure, however in order to quantify the change in capacitance relative to the severity of deformation we consider the differential average. This value can also be normalised by using the average baseline value as an offset. A mathematical representation of this approach for phase A is,

$$\bar{\Delta}_A = \Delta_A(X\%) - \Delta_A(0\%), \quad (6)$$

where

$$\Delta_A(X\%) = \left[\frac{|C_{Aai} - C_{Bbi}| + |C_{Aai} - C_{Cci}|}{2} \right]_{X\%}. \quad (7)$$

$\bar{\Delta}_A$ represents an independent value for the change in the interwinding capacitance of phase A due to ‘buckling’, noting that this approach is equally applicable to any phase. As per Section 3.2, for the ‘buckling’ conditions being considered here we would expect the interwinding capacitance differential average for phase A to increase with increased ‘buckle’. With reference to Table 3, the value of $\bar{\Delta}_A$ for each test case shows this to hold true.

Table 3 Differential interwinding capacitance values (relative to phase A) for each of the ‘Buckling’ tests

% ‘Buckling’	$\bar{\Delta}_A$
0 (Baseline)	0
8	+1.35
16	+3.80
24	+5.65

Table 4 Model and FEA estimates for the change in the phase A interwinding capacitance based on the emulation of outward radial ‘buckling’ for 0 (Baseline), 8, 16 and 24% of the winding circumference

% ‘Buckling’	% Change (model)	% Change (FEA)
0	–	–
8	+2	+3
16	+5	+6
24	+7	+9

To confirm that the degree of change in the interwinding capacitance is correct, the change relative to the baseline value is compared with that predicted by a FEA model of the problem using the COMSOL Multiphysics suite of software. The resulting FEA electrostatics model shown in Fig. 8, is comprised of coaxial cylinders representing the 1.3 MVA transformer’s HV and LV windings (red and dark blue in colour, respectively), a cylinder between the two windings which represents the insulation press board (light blue), and a cylindrical section to represent the added neoprene strips between the two windings (brown), and the model’s electric field lines (red arrows). The results are presented in Table 4. The estimated percentage change in the value of the capacitance relative to the amount of ‘buckling’ is very close to that predicted by FEA.

Whilst the results in this paper were determined using Gray Box modelling techniques on a modified power transformer, these results align well with the findings of researchers who have utilised White Box models and simulated deformation using FEA. Examples include [36] which tracked the interwinding capacitive changes relative to deformation, and the researchers in [35] who tracked the differential shift in frequency associated with winding deformation induced capacitive change.

6 Conclusion

The research presented in this paper used transformer modelling techniques in conjunction with FRA measurements to determine parameter changes within a transformer structure. The validity of the approach was demonstrated in the following manner. The first step was to record baseline FRA results for the transformer under consideration. Next a Gray Box model was fitted to the baseline FRA in order to determine the baseline model parameters. The third step was to introduce a winding ‘buckle’ into one phase of the transformer. The FRA tests were repeated and the Gray Box model fitting algorithm was applied to the post-buckle FRA results. The subtle variation in the model capacitance parameters were clearly indicative of the induced winding structural change, demonstrating the methodology’s potential. Whilst FRA has found widespread application as a tool that can be used to potentially identify winding deformation, this research has demonstrated experimentally how it can be used to quantify the severity of this deformation. It is proposed that this approach could be used to support an automated deformation detection algorithm within a commercial FRA package.

7 References

- Arshad, M., Islam, S.M., Khaliq, A.: ‘Power transformer aging and life extension’. Probabilistic Methods Applied to Power Systems, 2004 Int. Conf. on, 2004, pp. 498–501
- Arshad, M., Islam, S.M.: ‘Power transformer condition assessment using oil UV – spectrophotometry’. Electrical Insulation and Dielectric Phenomena, 2007. CEIDP 2007. Annual Report – Conf. on, 2007, pp. 611–614
- Prevost, T.A., Woodcock, D.J.E.: ‘Transformer fleet health and risk assessment’. IEEE PES Transformers Committee Tutorial 2007, Dallas, Texas, 2007
- Wang, M., Vandermaar, A.J., Srivastava, K.D.: ‘Review of condition assessment of power transformers in service’, *IEEE Electr. Insul. Mag.*, 2002, **18**, pp. 12–25
- Steiner, J.P., Weeks, W.L.: ‘A new method for locating partial discharges in transformers’. Conf. on Electrical Insulation and Dielectric Phenomena, 1990, Annual Report., 1990, pp. 275–281
- Bagheri, M., Naderi, M.S., Blackburn, T., *et al.*: ‘FRA vs. short circuit impedance measurement in detection of mechanical defects within large power transformer’. Electrical Insulation (ISEL), Conf. Record of the 2012 IEEE Int. Symp. on, 2012, pp. 301–305
- Wang, M., Vandermaar, A.J., Srivastava, K.D.: ‘Transformer winding movement monitoring in service – key factors affecting FRA measurements’, *IEEE Electr. Insul. Mag.*, 2004, **20**, pp. 5–12
- Lee, J.Y., Ahn, H.M., Kim, J.K., *et al.*: ‘Finite element analysis of short circuit electromagnetic force in power transformer’. Electrical Machines and Systems, 2009. ICEMS 2009. Int. Conf. on, 2009, pp. 1–4
- Abeywickrama, N., Serdyuk, Y.V., Gubanski, S.M.: ‘High-frequency modeling of power transformers for use in frequency response analysis (FRA)’, *IEEE Trans. Power Deliv.*, 2008, **23**, pp. 2042–2049
- Bagheri, M., Naderi, M.S., Blackburn, T., *et al.*: ‘Frequency response analysis and short-circuit impedance measurement in detection of winding deformation within power transformers’, *IEEE Electr. Insul. Mag.*, 2013, **29**, p. 7
- Dick, E.P., Erven, C.C.: ‘Transformer diagnostic testing by frequency response analysis’, *IEEE Trans. Power Appar. Syst.*, 1978, **PAS-97**, pp. 2144–2153
- Kraetge, A., Kruger, M., Fong, P.: ‘Frequency response analysis - Status of the worldwide standardization activities’. Condition Monitoring and Diagnosis, 2008. CMD 2008. Int. Conf. on, 2008, pp. 651–654
- Ryder, S.A.: ‘Diagnosing transformer faults using frequency response analysis’, *IEEE Electr. Insul. Mag.*, 2003, **19**, pp. 16–22
- Behjat, V., Vahedi, A., Setayeshmehr, A., *et al.*: ‘Diagnosing shorted turns on the windings of power transformers based upon online FRA using capacitive and inductive couplings’, *IEEE Trans. Power Deliv.*, 2011, **26**, pp. 2123–2133
- Bjerkkan, E.: ‘High frequency modeling of power transformers – stresses and diagnostics’ (Faculty of Information Technology, Mathematics and Electrical Engineering, 2005)
- ‘Mechanical condition assessment of transformer windings using Frequency Response Analysis (FRA)’, ELECTRA-CIGRE WG A2.26 Report 342, April 2008, vol. 237
- Luo, Y., Gao, J., Chen, P., *et al.*: ‘A test method of winding deformation excited by pseudorandom M-Sequences — Part I: theory and simulation’, *IEEE Trans. Dielectr. Electr. Insul.*, 2016, **23**, pp. 1605–1612
- Bigdeli, M., Vakilian, M., Rahimpour, E.: ‘Transformer winding faults classification based on transfer function analysis by support vector machine’, *IET Electr. Power Appl.*, 2012, **6**, pp. 268–276
- Bigdeli, M., Vakilian, M., Rahimpour, E.: ‘A probabilistic neural network classifier-based method for transformer winding fault identification through its transfer function measurement’, *Int. Trans. Electr. Energy Syst.*, 2013, **23**, pp. 392–404
- Karami, H., Gharehpetian, G.B., Norouzi, Y., *et al.*: ‘GLRT-based mitigation of partial discharge effect on detection of radial deformation of transformer HV winding using SAR imaging method’, *IEEE Sens. J.*, 2016, **16**, pp. 7234–7241
- Mitchell, S.D., Siegel, M., Beltle, M., *et al.*: ‘Discrimination of partial discharge sources in the UHF domain’, *IEEE Trans. Dielectr. Electr. Insul.*, 2016, **23**, pp. 1068–1075
- Rahimpour, E., Christian, J., Feser, K., *et al.*: ‘Transfer function method to diagnose axial displacement and radial deformation of transformer windings’, *IEEE Trans. Power Deliv.*, 2003, **18**, pp. 493–505
- Abeywickrama, K.G.N.B., Podoltsev, A.D., Serdyuk, Y.V., *et al.*: ‘Computation of parameters of power transformer windings for use in frequency response analysis’, *IEEE Trans. Magn.*, 2007, **43**, pp. 1983–1990
- Islam, S.M.: ‘Detection of shorted turns and winding movements in large power transformers using frequency response analysis’. IEEE Power Engineering Society Winter Meeting, 2000. January 2000, vol. 3, pp. 2233–2238
- Sofian, D.M., Wang, Z.D., Jarman, P.: ‘Interpretation of transformer FRA measurement results using winding equivalent circuit modelling technique’. Electrical Insulation and Dielectric Phenomena, 2005. CEIDP ‘05. 2005 Annual Report Conf. on, October 2005, pp. 613–616
- Jayasinghe, J.A.S.B., Wang, Z.D., Jarman, P.N., *et al.*: ‘Investigations on sensitivity of FRA technique in diagnosis of transformer winding deformations’. Electrical Insulation, 2004. Conf. Record of the 2004 IEEE Int. Symp. on, 2004, pp. 496–499
- Tang, W.H., Shintemirov, A., Wu, Q.H.: ‘Detection of minor winding deformation fault in high frequency range for power transformer’. Power and Energy Society General Meeting, 2010 IEEE, 2010, pp. 1–6
- Samimi, M.H., Tenbohlen, S., Shayegani Akmal, A.A., *et al.*: ‘Improving the numerical indices proposed for the FRA interpretation by including the phase response’, *Int. J. Electr. Power Energy Syst.*, 2016, **83**, pp. 585–593
- Yousof, M.F.M., Ekanayake, C., Saha, T.K.: ‘Frequency response analysis to investigate deformation of transformer winding’, *IEEE Trans. Dielectr. Electr. Insul.*, 2015, **22**, pp. 2359–2367
- Mitchell, S.D., Welsh, J.S.: ‘Initial parameter estimates and constraints to support gray box modeling of power transformers’, *IEEE Trans. Power Deliv.*, 2013, **28**, pp. 2411–2418
- Mitchell, S.D., Welsh, J.S.: ‘Modeling power transformers to support the interpretation of frequency-response analysis’, *IEEE Trans. Power Deliv.*, 2011, **26**, pp. 2705–2717
- Jayasinghe, J.A.S.B., Wang, Z.D., Jarman, P.N.: ‘Winding movement in power transformers: a comparison of FRA measurement connection methods’, *IEEE Trans. Dielectr. Electr. Insul.* [see also *IEEE Trans. Electr. Insul.*], 2006, **13**, pp. 1342–1349
- Karimifard, P., Gharehpetian, G.B.: ‘A new algorithm for localization of radial deformation and determination of deformation extent in transformer windings’, *Electr. Power Syst. Res.*, 2008, **78**, pp. 1701–1711

- 34 Ji, T.Y., Tang, W.H., Wu, Q.H.: 'Frequency response analysis of power transformer winding deformation based on a hybrid model'. Power Engineering and Automation Conf. (PEAM), 2011 IEEE, 2011, vol. 3, pp. 144–147
- 35 Hashemnia, N., Abu-Siada, A., Islam, S.: 'Improved power transformer winding fault detection using FRA diagnostics part 2: radial deformation simulation', *IEEE Trans. Dielectr. Electr. Insul.*, 2015, **22**, pp. 564–570
- 36 Zhang, Z.W., Tang, W.H., Ji, T.Y., *et al.*: 'Finite-element modeling for analysis of radial deformations within transformer windings', *IEEE Trans. Power Deliv.*, 2014, **29**, pp. 2297–2305
- 37 Thomas, P.H.: 'Static strains in high tension circuits and the protection of apparatus', *Trans. Am.Inst.Electr.Eng.*, 1902, **XIX**, pp. 213–264
- 38 Rohrer, R.A.: 'Circuit theory: an introduction to the state variable approach' (McGraw-Hill, 1970)
- 39 Kojima, H., Miyata, H., Shida, S., *et al.*: 'Buckling strength analysis of large power transformer windings subjected to electromagnetic force under short circuit', *IEEE Trans. Power Appar.Syst.*, 1980, **PAS-99**, pp. 1288–1297
- 40 Bhel, S.S.: 'Transformers' (Tata McGraw-Hill, 2003)
- 41 Kulkarni, S.V., Khaparde, S.A.: 'Transformer engineering: design and practice' (Marcel Dekker, 2004)
- 42 Steel, R.B., Johnson, W.M., Narbus, J.J., *et al.*: 'Dynamic measurements in power transformers under short circuit conditions' (CIGRE, 1972)
- 43 Cheng, D.K.: 'Field and wave electromagnetics' (Addison-Wesley, 1983)